The Journal of Neuroscience, October 15, 1996, *16*(20):6374–6385

$GABA_B$ Receptor-Activated Inwardly Rectifying Potassium Current in Dissociated Hippocampal CA3 Neurons

Deborah L. Sodickson and Bruce P. Bean

Vollum Institute, Oregon Health Sciences University, Portland, Oregon 97201, and Program in Neuroscience, Harvard Medical School, Boston, Massachusetts 02115

GABA and the $GABA_B$ receptor agonist baclofen activated a potassium conductance in acutely dissociated hippocampal CA3 neurons. Baclofen-activated current required internal GTP, was purely potassium selective, and showed strong inward rectification. As with acetylcholine-activated current in atrial myocytes, external Cs^+ blocked inward but not outward current in a highly voltage-dependent manner, whereas Ba^{2+} blocked with no voltage dependence. Unlike the cardiac current, however, the baclofen-activated current showed no intrinsic voltage-dependent relaxation. With fast solution exchange, current was activated by baclofen or GABA with a lag of ~50 msec followed by an exponential phase (time constant ~225 msec at saturating agonist concentrations); deactivation was preceded by a lag of ~150 msec and occurred with a time constant of ~1 sec. GABA activated the potassium conductance with a half maximally effective concentration (EC_{50}) of 1.6 μM, much lower than that for activation of $GABA_A$ receptor-activated chloride current in the same cells (EC_{50} ~25 μM). At low GABA concentrations, activation of the $GABA_B$ current had a Hill coefficient of 1.4–2.1, suggesting cooperativity in the receptor-to-channel pathway. Although the maximal conductance activated by $GABA_B$ receptors is much smaller than that activated by $GABA_A$ receptors, its higher sensitivity to GABA and slower time course make it well suited to respond to low concentrations of extra-synaptic GABA.

Key words: baclofen; G-protein; GIRK; GABA; $GABA_A$; chloride current; cesium; barium

Two major postsynaptic conductances activated by GABA exist in central neurons. One is a chloride conductance activated by $GABA_A$ receptors and is present in virtually all central neurons. The second is a less widely distributed potassium conductance activated by $GABA_B$ receptors (Gähwiler and Brown, 1985; Newberry and Nicoll, 1985; Dutar and Nicoll, 1988). In neurons that possess both receptors postsynaptically, the requirements for activation are often strikingly different, with $GABA_B$-mediated inhibitory postsynaptic potentials requiring stronger or more sustained stimulation than $GABA_A$-mediated responses (Dutar and Nicoll, 1988; Otis and Mody, 1992). The reasons for this are not clearly understood.

In hippocampal pyramidal neurons, the $GABA_B$-activated potassium conductance is inwardly rectifying (Gähwiler and Brown, 1985) and mediated by G-proteins (Andrade et al., 1986; Thalmann, 1988; Thompson and Gähwiler, 1992a) and can be blocked by external Ba^{2+} ions (Newberry and Nicoll, 1985; Misgeld et al., 1989). These properties are shared by transmitter-activated potassium currents present in various other neurons (North et al., 1987; North, 1989; Nicoll et al., 1990) as well as in cardiac atrial myocytes, where detailed characterization has been possible (Hartzell, 1988). A family of cDNAs encoding subunits of G-protein-activated inward-rectifier potassium (GIRK) channels has been described (Dascal et al., 1993; Kubo et al., 1993; Lesage et al., 1994; Doupnik et al., 1995; Krapivinsky et al., 1995b). Both native channels and cloned channels seem to be activated by binding of $\beta\gamma$ subunits of G-proteins (Logethetis et al., 1987; Reuveny et al., 1994; Wickman et al., 1994; Huang et al., 1995; Inanobe et al., 1995; Krapivinsky et al., 1995b; Oh et al., 1995). G-protein α subunits may modulate the activation (Schreibmayer et al., 1996) or help mediate coupling to specific transmitter receptors (Huang et al., 1995).

Detailed characterization of the $GABA_B$-activated potassium channels in hippocampal neurons has been hindered by lack of a suitable single-cell preparation. Experiments using tissue slices are limited by the difficulty of making rapid solution changes. For unknown reasons, the conductance is absent or minimal in conventional hippocampal tissue culture preparations (Harrison, 1990; Yoon and Rothman, 1991; Pfrieger et al., 1994), although it is preserved in organotypic cultures (Gähwiler and Brown, 1985). Even such basic properties as the dose–response relationship for GABA and kinetics of current activation are unknown. Knowledge of such properties should help in understanding the differences in synaptic activation of $GABA_A$ and $GABA_B$ receptors.

Acutely isolated cells have been used previously to study serotonin-activated potassium current in dorsal raphe neurons (Penington et al., 1993a). Stimulated by this, we found that robust $GABA_B$ receptor-activated potassium currents can be recorded in a preparation of acutely dissociated hippocampal CA3 neurons that permits rapid solution changes. We characterized the kinetics, rectification, ionic block, and GABA dependence of the current. The results show that the slow kinetics of $GABA_B$-mediated inhibitory postsynaptic currents are primarily attributable to kinetics of receptor-to-channel coupling and that activation of

Received May 31, 1996; revised July 26, 1996; accepted July 30, 1996.

This work was supported by National Institutes of Health Grant HL35034. We thank David Cardozo for advice, and Gabriela Greif, Craig Jahr, Stefan McDonough, Indira Raman, Gary Westbrook, and John Williams for comments on this manuscript.

Correspondence should be addressed to Deborah Sodickson, Volen Center, Brandeis University, 415 South Street, Waltham, MA 02254.

Bruce Bean's present address: Department of Neurobiology, Harvard Medical School, 220 Longwood Avenue, Boston, MA 02115.

$GABA_B$ receptors requires very low levels of extracellular GABA, perhaps near background levels.

MATERIALS AND METHODS

Preparation of freshly dissociated neurons. Hippocampi from 7- to 12-d-old Long Evans rats were dissected in ice-cold, oxygenated dissociation solution containing (in mM): 82 Na_2SO_4, 30 K_2SO_4, 5 $MgCl_2$, 10 HEPES, 10 glucose, and 0.001% phenol red indicator, pH 7.4. Slices were cut 400 μM thick and incubated for 9 min at 37°C in dissociation solution containing 3 mg/ml protease (Type XXIII, Sigma, St. Louis, MO). Enzyme solution was then replaced with dissociation solution containing 1 mg/ml trypsin inhibitor and 1 mg/ml bovine serum albumin, and the slices were allowed to cool to room temperature under an oxygen atmosphere. As cells were needed, slices were withdrawn, and the CA3 region was dissected out and triturated to release individual cells. Cells were placed in the recording chamber in Tyrode's solution containing (in mM): 150 NaCl, 4 KCl, 2 $CaCl_2$, 2 $MgCl_2$, 10 glucose, and 10 HEPES, pH 7.4 with NaOH. Cells were used within 6–8 hr of slice preparation.

CA3 pyramidal neurons were identified morphologically, based on size and shape. Cells identified as pyramidal neurons had a large pyramidal-shaped cell body (12–16 μ width, 20–36 μ length) with a thick apical dendritic stump (4–6 μ width, 18–24 μ length) and, in some neurons, one to four basal dendritic stumps (1–4 μ width, 6–14 μ length). Average cell capacitance was 23 ± 5 pF (n = 125; range, 15–38 pF). Despite the presence of dendritic stumps, the cells behaved as if they were electrotonically compact: capacity transients settled with a single time constant of 200–350 μsec.

Whole-cell voltage-clamp recordings. Patch pipettes were pulled from 100 μl Boralex micropipettes (Dynalab, Rochester, NY.). Pipette resistances ranged from 2 to 5 MΩ when filled with internal solution containing (in mM): 108 KH_2PO_4, 4.5 $MgCl_2$, 9 HEPES, 9 EGTA, 14 mM creatine phosphate (Tris salt), 4 mM Mg-ATP, and 0.3 mM GTP (Tris salt), pH adjusted to 7.4 with 135.4 mM KOH. The creatine phosphate ATP and GTP were added from 10× concentrated aliquots stored at −70°C. To prevent nucleotide hydrolysis, the final internal solution was kept on ice after phosphates were added.

The liquid junction potential between the internal solution and Tyrode's solution (in which the current was zeroed before obtaining a seal) was −12 mV, measured as described by Neher (1992). Membrane potentials were corrected for this junction potential.

Seals were formed and the whole-cell configuration was obtained in bath Tyrode's solution. The cell was then bathed by a gravity-driven, constant stream of external solution flowing through microcapillary perfusion pipes positioned directly in front of the cell. The perfusion pipes consisted of a linear array of 12 microcapillary tubes of internal diameter 200 μ or 250 μ, glued together side by side and fed from separate reservoirs. Solutions were changed by moving the perfusion pipes. In some experiments, the cell was lifted from the bottom of the chamber, and solution changes were made under computer control by using a solenoid attached to the recording pipette to rapidly move the cell between adjacent pipes. The speed of solution exchanges made by this method (used for the experiments in Figs. 8–13) was measured by the time course of current relaxation when the $GABA_B$-activated conductance was activated by steady application of 10–100 μM baclofen and the cell was moved between solutions containing 60 mM and 16 mM K^+. The time constant of solution change varied between 3 and 20 msec in different cells.

External recording solutions consisted of modified Tyrode's solution with 4–60 mM KCl, with KCl substituted for an equimolar amount of NaCl. Tetrodotoxin (TTX) was included at 2–3 μM in all solutions to block sodium currents. R(+)-baclofen, GABA, GTP-γ-S, GDP-β-S, and ω-conotoxin MVIIC were stored as concentrated aliquots at −70°C or −20°C and diluted into recording solution on the day of the experiment. Whole-cell currents were recorded with an Axopatch 200A patch-clamp amplifier, filtered at 2 kHz, digitized at 20–50 KHz, and stored using a BASIC-FASTLAB analog/digital interface and software (Indec Systems, Sunnyvale, CA) or a Digidata interface and PClamp6 software (Axon Instruments, Foster City, CA).

Current–voltage curves. Current–voltage curves were determined using voltage ramps from −172 mV to +8 mV, 100 msec in duration. To smooth the voltage signal, it was low-pass filtered at 0.5 kHz (4-pole Bessel filter) before being applied to the patch-clamp amplifier. The voltage was corrected for the delay resulting from the filtering. Baclofen-induced current was obtained by subtracting ramp currents before and after application of baclofen, as shown in Figure 3. In hippocampal CA3 neurons, baclofen inhibits voltage-dependent calcium current as well as activating potassium current. This effect overlaps with the baclofen-activated K current at potentials positive to −40 mV, where calcium current begins to be activated. We initially used Cd^{2+} to block calcium currents, but found that the inward rectifier K current was also reduced (~50% block with 100 μM Cd^{2+}). Nimodipine and nicardipine, which block L-type calcium current, were also found to partially block the baclofen-activated K current (~60% block by 10 μM nimodipine and ~60% block by 3 μM nicardipine). The peptide ω-conotoxin MVIIC inhibits at least three components of calcium current in CA3 neurons (McDonough et al., 1996), and the calcium current that remains has little or no sensitivity to short applications of baclofen (K. J. Swartz and B. P. Bean, unpublished observations). ω-Conotoxin MVIIC (10 μM) was therefore included in all external solutions in experiments measuring reversal potentials.

All statistics are given as mean ± SEM.

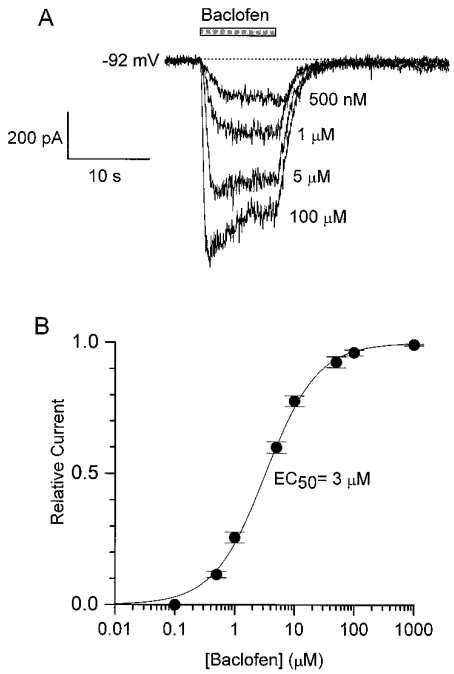

Figure 1. Dose-dependent activation of current by baclofen applied to hippocampal CA3 neurons. *A*, Inward current elicited at a holding potential of −92 mV by successive application of 500 nM, 1 μM, 5 μM, and 100 μM baclofen, with 60 mM external K^+ and 243 mM internal K^+. *B*, Dose–response relationship for baclofen activation of current. Symbols and error bars represent mean ± SEM for determinations in nine cells for 500 nM to 1 mM baclofen and four cells for 100 nM baclofen. The response at each baclofen concentration was normalized to the maximal response obtained with 100 μM or 1 mM baclofen. The full series of seven or eight agonist concentrations was preceded and followed by applications of 50 μM baclofen, and results were used only if these responses differed by <20%. The *line* is the best least-squares fit to $1/(1 + EC_{50}/[\text{baclofen}])$, where EC_{50} is the half-maximally effective concentration of baclofen. EC_{50} = 3 μM. External solution: 60 mM KCl, 94 mM NaCl, 2 mM $CaCl_2$, 10 mM HEPES, 2 mM $MgCl_2$, 10 mM glucose, pH 7.4 with KOH, 3 μM TTX.

RESULTS

Dose dependence

Initial experiments were carried out with baclofen rather than GABA to avoid activating $GABA_A$ receptors. Baclofen activated inwardly rectifying potassium current in 401 of 402 neurons tested. Figure 1 shows the dose dependence of the baclofen-activated current. Substantial current was activated by baclofen concentrations of 500 nM and above. The dose–response relationship for baclofen could be fit fairly well by the logistic equation with an EC_{50} of 3 μM and a Hill coefficient of 1 (Fig. 1*B*). Despite the presence in the cells

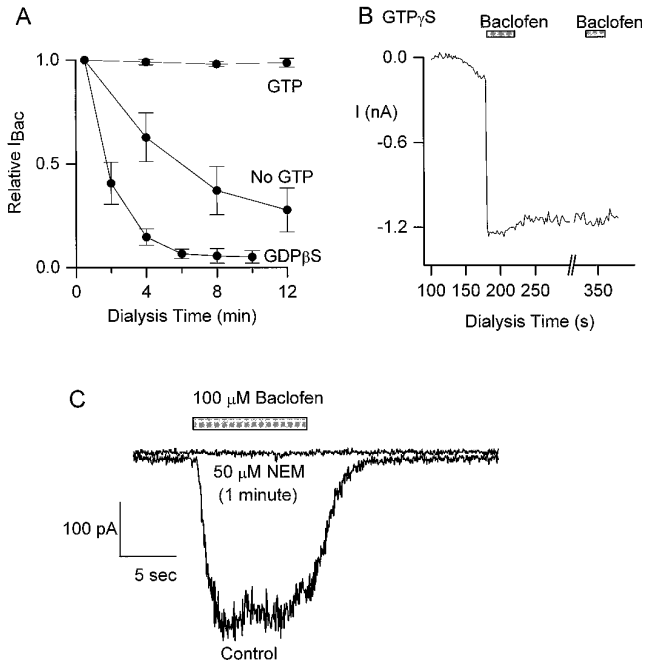

Figure 2. Guanyl nucleotide dependence of the baclofen-induced current. *A*, Decline in baclofen response over time with standard pipette GTP (300 μM), no GTP, and 800 μM GDPβS. Time 0 is the time at which the whole-cell configuration was attained. Current at each time point is normalized to the initial baclofen response examined 30 sec after attaining whole-cell recording. Points are mean ± SEM from determinations in five cells for GTP, eight cells with no GTP, and 10 cells with 800 μM GDPβS. Cells were held at −92 mV and studied with 60 mM K^+ Tyrode's solution. *B*, Effect of 300 μM intracellular GTPγS. After 3 min of GTPγS dialysis, 50 μM baclofen was applied. The response did not reverse, and a second baclofen application 2.5 min later produced no further response. The cell was held at −92 mV and studied with 60 mM K^+ Tyrode's solution. *C*, Effect of NEM on baclofen activation of current. Current was elicited from a holding potential of −92 mV with 50 μM baclofen; 50 μM NEM was applied for 1 min. External solution: 60 mM K^+ Tyrode's solution.

of large chloride conductances that could be activated by $GABA_A$ receptors (see Figs. 13, 14), baclofen up to 1 mM had perfect selectivity for the $GABA_B$-mediated response. With applications of 100 μM or higher, the baclofen-activated current began to decline or desensitize after ~1 sec (Fig. 1*A*).

Dependence on GTP

Our standard pipette solution included 300 μM GTP. To test the GTP dependence of the baclofen response, we omitted pipette GTP or replaced it with nonhydrolyzable GTP and GDP analogs (Fig. 2*A,B*). If GTP was omitted from the pipette solution, the baclofen-induced current fell to 28 ± 11% (n = 8) of the initial current after 12 min of dialysis. If the GDP analog GDPβS was included in the pipette solution (at 800 μM), the baclofen-induced current disappeared faster, falling to <5% in 4–12 min of dialysis in 12 of 14 cells tested. When the poorly hydrolyzable GTP analog GTPγS (300 μM) was included in the pipette solution, a small inward current began to appear after 2–3 min of dialysis, even in the absence of baclofen. If baclofen was then applied, a large current was activated promptly and irreversibly (Fig. 2*B*). A second baclofen application produced no further response. Similar irreversible responses were obtained in 11 of 11 cells tested with GTPγS. These experiments suggest that the coupling between $GABA_B$ receptors and potassium channels is dependent on GTP acting via G-proteins.

In hippocampal slices, baclofen activation of potassium current can be prevented by intracerebral injections of pertussis toxin (Andrade et al., 1986; Andrade and Nicoll, 1987; Thalmann, 1988; Thompson and Gähwiler, 1992a). We tested the ability of pertussis toxin to disrupt the receptor-channel coupling in dissociated neurons, but with inconclusive results. With inclusion of the catalytic subunit (A-protomer, 5 μg/ml, preactivated by 20 mM DTT) in the pipette solution, along with its substrate NAD (1 mM), the baclofen-activated current declined slowly with time, with a 30–55% reduction in current (n = 4) after up to 45 min of dialysis. We used the same procedure in rat atrial myocytes and also found only slow decline in the acetylcholine-activated current, even though the atrial muscarinic response in various species is completely sensitive to pertussis toxin applied overnight or to excised patches (Pfaffinger et al., 1985; Kurachi et al., 1986a,b; Ito et al., 1991). We conclude that under our conditions the procedure is not adequate for testing the pertussis toxin sensitivity of the transduction pathway.

When applied for short times, the sulfhydryl alkylating agent *N*-ethyl-maleimide (NEM) specifically eliminates responses mediated by pertussis toxin-sensitive G-proteins, whereas it spares responses by other G-proteins (Nakajima et al., 1990; Wollmuth et al., 1995). Figure 2*C* shows the effect of 50 μM NEM on the baclofen-activated current in hippocampal neurons. With a 1 min extracellular application, the baclofen response was abolished completely. This result was obtained in four of the four cells tested. Although this result is far from a definitive test of mediation of the response by pertussis toxin-sensitive G-proteins, the rapid and complete effects of NEM raise the possibility that lower concentrations could be used as a tool to modify receptor-to-channel coupling in a titratable manner.

Inward rectification

Figure 3 shows the current–voltage relationship for the baclofen-activated K current under quasi-physiological ionic conditions, with 4 mM external K^+ and 243 mM internal K^+. In contrast to serotonin-activated current in acutely dissociated dorsal raphe neurons (Penington et al., 1993a), it was easy to record currents with physiological external K^+ concentrations. Current–voltage curves were obtained using a voltage ramp from −172 mV to +8 mV. The ramp was kept relatively short (100 msec) to minimize the time at voltages positive to −50 mV, where large voltage- and time-dependent potassium currents are activated. The baclofen-induced current reversed at −90 mV and was strongly inwardly rectifying, with inward current at −150 mV (carried by 4 mM K^+), approximately three times larger than the outward current at −50 mV (carried by 243 mM K^+). Despite the powerful rectification, however, the baclofen-induced outward current was substantial compared with basal currents at potentials of −80 to −40 mV, the range of typical neuronal resting potentials. In the cell of Figure 3, the zero current potential (which would correspond to the resting potential if the cell were not voltage-clamped) was hyperpolarized from −44 mV to −53 mV by baclofen. Thus, the outward potassium current is large enough to have a significant hyperpolarizing effect.

Potassium dependence

Figure 4 shows the dependence of the baclofen-activated current on external potassium concentration, determined in a single neuron. As potassium was increased from 4 to 60 mM, the inward current increased dramatically, and the reversal potential shifted almost exactly as predicted by the Nernst equation

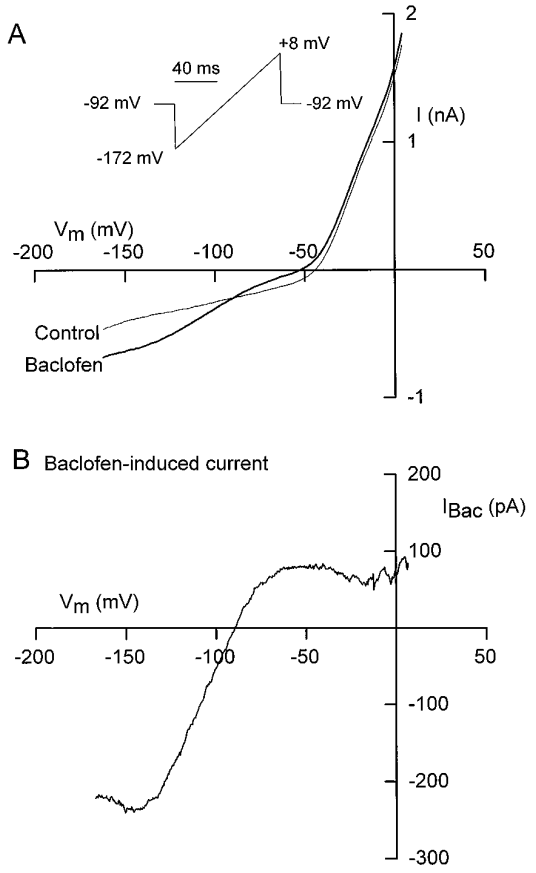

Figure 3. Current–voltage relationship of the baclofen-activated current determined with 4 mM external K^+. *A*, Current was measured in the absence and presence of 50 μM baclofen at voltages from −172 to +8 mV, varied by a voltage ramp lasting 100 msec (*inset*). Current traces are signal-averaged from 11 traces for control and 17 traces for baclofen and are corrected for capacitative current (determined from the transient for the initial step from −92 to −172 mV). *B*, Baclofen-sensitive current obtained by subtraction of the traces in *A*.

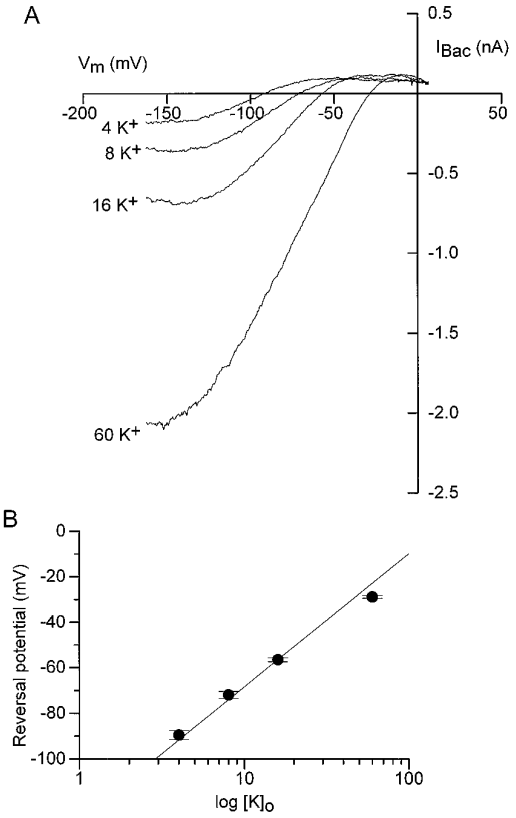

Figure 4. Dependence on external K^+ of the magnitude and reversal potential of the baclofen-activated current. *A*, Current–voltage relationships for the baclofen-induced current from a single cell with 4, 8, 16, and 60 mM external K^+. Each trace is the difference between current in 50 μM baclofen (signal-averaged from 11–16 traces) and control current (signal-averaged from 12–15 traces). Reversal potentials for baclofen-induced current are −92 mV with 4 mM K^+, −71 mV with 8 mM K^+, −57 mV with 16 mM K^+, and −28 mV with 60 mM K^+. *B*, Reversal potential as a function of external K^+. Symbols and error bars represent mean ± SEM for determinations in six cells at each concentration. The *solid line* is the Nernst potassium equilibrium potential $(RT/F)*\ln(0.45*[K^+]_{out}/0.75*[K^+]_{in})$, with $[K^+]_{in}$ = 243 mM and T = 22°C. The activity coefficients for the external solution (0.45) and internal solution (0.75) were estimated based on the tables given by Robinson and Stokes (1959) for K_2HPO_4 and NaCl, respectively. External solutions: Tyrode's solution with equimolar substitution of KCl for NaCl to obtain desired KCl concentration. ω-Conotoxin MVIIC (10 μM) was included in all external solutions to block voltage-dependent calcium currents, which are reduced by baclofen and could distort baclofen-induced currents at potentials positive to approximately −40 mV.

for a purely potassium-selective conductance. As is characteristic of inwardly rectifying potassium channels (Hille, 1992a), the voltage dependence of rectification depended on V_m-E_k as external potassium was altered. At strongly negative voltages (below approximately −140 mV), inward current saturated. This saturation disappeared in Na-free external solutions (not shown). The saturation is likely attributable to voltage-dependent block by external Na^+ ions, as has been described for other inward rectifiers (Ohmori, 1978; Standen and Stanfield, 1979; Harvey and Ten Eick, 1989).

Block by external Cs^+ and Ba^{2+}

Baclofen-induced current was blocked by external Cs^+ and Ba^{2+} ions. With 4 mM external K^+, Cs^+ blocked inward current in a highly voltage-dependent manner and had no effect on outward current at concentrations up to 3 mM (Fig. 5*A*). At any given voltage, the concentration dependence of Cs^+ block could be fit well by a Langmuir isotherm (Fig. 5*B*), with a half-blocking concentration that increased exponentially from ~30 μM at −162 mV to ~200 μM at −122 mV, corresponding to an e-fold change every 10 mV. In another series of experiments using 16 mM external potassium, the half-blocking concentration of Cs^+ was slightly lower than for 4 mM K^+ at voltages positive to −150 mV (as if the cesium ion was "trapped" by the higher external K^+), but the IC_{50} at voltages negative to −150 mV saturated at ~40 μM Cs^+ (Fig. 5*C*).

Block by Ba^{2+} was very different. It showed no voltage dependence, with outward current blocked equally as well as inward current (Fig. 6). At all voltages, the dose dependence of inhibition could be fit well by a Langmuir isotherm with an IC_{50} of 12 μM (Fig. 6*B*). The experiment in Figure 6*A* was carried out with a fast ramping protocol that in principle might allow too little time for relaxation of voltage-dependent block; however, there was also no voltage dependence evident when it was tested with voltage steps lasting 2–5 sec (not shown). In contrast to Cs^+ block, a fourfold increase in external K^+ concentration had no effect on block by Ba^{2+}, regardless of voltage (Fig. 6*C*).

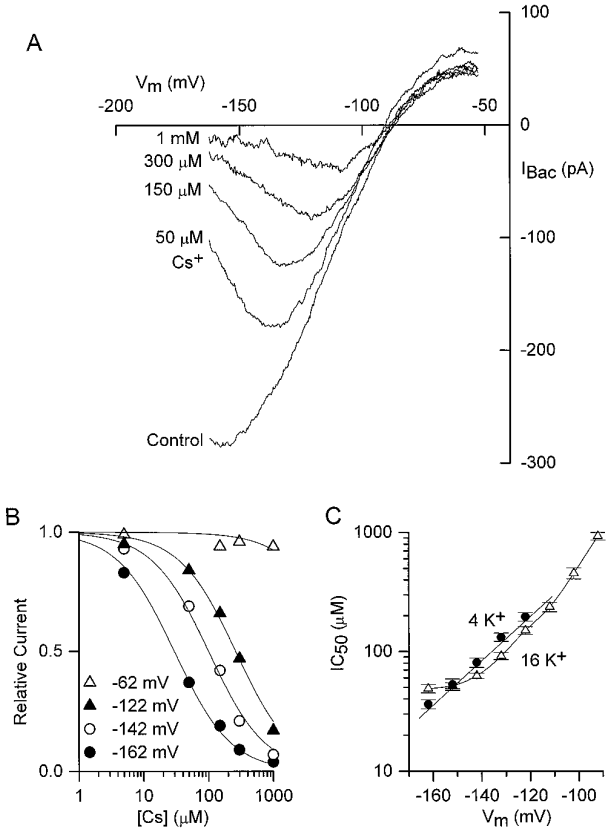

Figure 5. Voltage-dependent Cs^+ block of the baclofen response. *A*, Block of the baclofen-induced current in a single cell by 50 μM, 150 μM, 300 μM, and 1 mM Cs^+. Cs^+ was present in both control and baclofen-containing solutions. Current traces were signal-averaged (8–11 traces for control, 12–16 traces for baclofen) before subtraction. *B*, Voltage dependence of Cs^+ block from the same cell as in *A*. Baclofen response at each Cs^+ concentration was normalized to the baclofen response in the absence of Cs^+. *Solid curves* are least-squares fits to the expression $1/(1 + [Cs^+]/IC_{50})$, where IC_{50} is the half-maximally effective dose of Cs^+ (246 μM at −132 mV, 92 μM at −152 mV, and 31 μM at −172 mV). *C*, Voltage dependence of Cs^+ block with 4 mM and 16 mM external K^+. *Points* show mean IC_{50} (± SEM) determined as in Figure 5 for seven cells with 4 mM K^+ (*circles*) and eight cells with 16 mM K^+ (*triangles*).

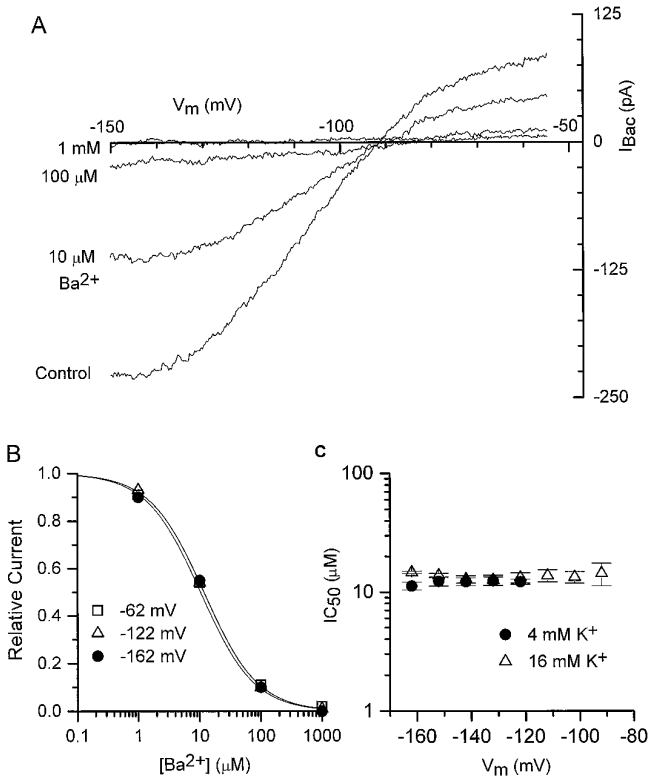

Figure 6. Ba^{2+} block of the baclofen response in 4 mM external K^+. *A*, Block of the baclofen-induced current in a single cell by 10 μM, 100 μM, and 1 mM Ba^{2+}. $BaCl_2$ was added to both control and baclofen-containing solutions. Each trace is the control-subtracted response to 50 μM baclofen. Before subtraction, current traces were signal-averaged (8–10 traces for controls, 14–17 traces for baclofen). *B*, Lack of voltage dependence of block by Ba^{2+}. Baclofen response at each Ba^{2+} concentration was normalized to the baclofen response in the absence of Ba^{2+}. Same cell as in *A*. *Solid curves* are fits to the equation $1/(1 + [Ba^{2+}]/IC_{50})$, where IC_{50} is the concentration of Ba^{2+} giving half-block (IC_{50} = 13 μM at −62 mV, and 12 μM at −122 and −162 mV). *C*, IC_{50} as a function of voltage for experiments with 4 mM (*circles*, n = 9) or 16 mM (*triangles*, n = 3) external K^+.

Lack of time-dependent gating

Many inwardly rectifying potassium channels display time- and voltage-dependent components of current (for review, see Hille, 1992a). Such voltage-dependent relaxations are seen with the potassium conductance activated by muscarinic receptors in most cardiac atrial cells (Noma and Trautwein, 1978; Sakmann et al., 1983; Simmons and Hartzell, 1987; but see Carmeliet and Mubagwa, 1986). We tested for voltage-dependent relaxations using long hyperpolarizations (Fig. 7). In contrast to the results in cardiac cells, there was no resolvable time-dependent relaxation in the baclofen-induced current. This result was obtained both in physiological K^+ with a step from −72 mV to −132 mV (Fig. 7*A*) and in 60 mM K^+ with a step from −12 mV to −132 mV (Fig. 7*B*).

Kinetics of activation and deactivation

The kinetics of current activation on exposure to baclofen depended on the baclofen concentration. Maximal current occurred at ~3-5 sec with application of 5 μM baclofen and at ~1 sec with application of 100 μM baclofen. In experiments in which rapid solution changes were made under computer control, current was seen to rise with a sigmoidal time course (Fig. 8*A*). The final two thirds of the rising phase could be fit well by an exponential, with a time constant that declined from ~600 msec at 5 μM baclofen to ~250 msec at 100 μM baclofen (Fig. 8*A*). In the collected results shown in Figure 8*B*, it can be seen that increasing the baclofen concentration from 100 μM to 1 mM produced little further acceleration of kinetics, suggesting that the asymptotic value of 225 msec reflects a rate-limiting step subsequent to binding of agonist to receptor. On removal of baclofen, the decline of current was also sigmoidal. After an initial delay, the decline of current could be fit well with a single exponential (Fig. 8*A*). The time constant of decay ranged from ~450 msec to 2 sec among individual cells; the average time constant was 1.1 ± 0.1 sec (n = 38).

Figure 9 shows with higher resolution the sigmoidicity of activation and deactivation. The cell was moved between solutions with a computer-driven solenoid. The time course of solution change at the membrane of the cell was determined by the relaxation of current when the cell was moved between two solutions, both containing baclofen but having different K^+ concentration (thin traces); solution exchange was complete in ~10 msec. On application of agonist, there was a lag of ~50 msec before any significant activation of current (Fig. 9*A*). On removal

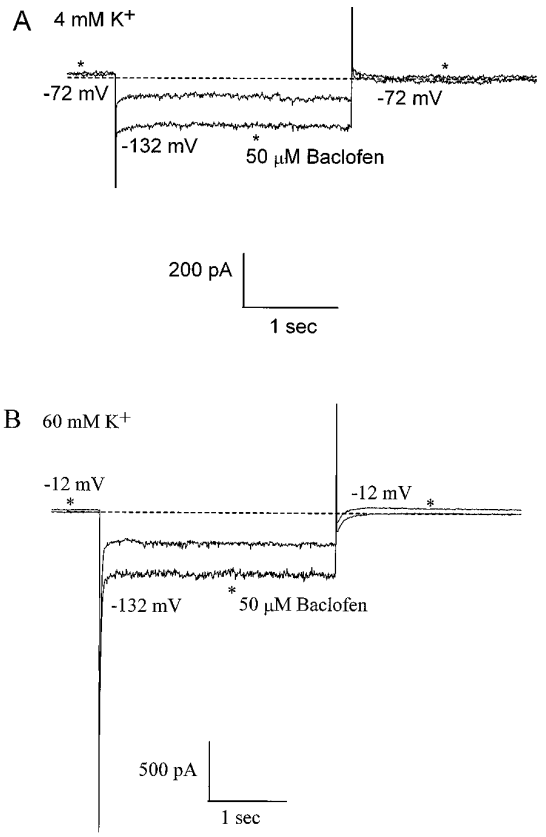

Figure 7. Lack of time dependence of the baclofen-induced K^+ current. *A*, With 4 mM external K^+, the cell was stepped from a holding potential of −72 mV to −132 mV. *Trace* marked by *asterisks* recorded in continuous presence of 50 μM baclofen. *B*, With 60 mM external K^+, a different cell was stepped from a holding potential of −12 mV to −132 mV.

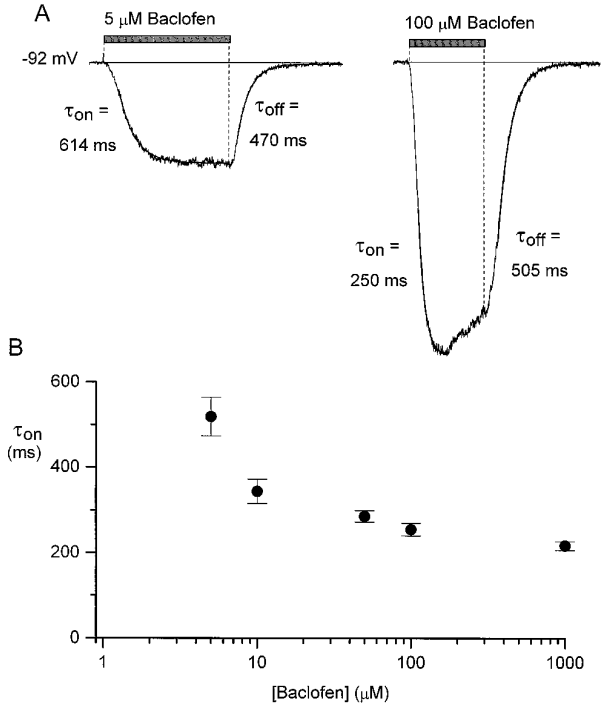

Figure 8. Kinetics of current activation and deactivation at different baclofen concentrations. *A*, Inward current elicited at a holding potential of −92 mV by computer-controlled application of 5 μM baclofen for 5 sec and 100 μM baclofen for 3 sec. To reduce noise from channel fluctuations, the responses were signal-averaged from five applications. *Thicker solid lines* overlying data traces are best fits of single exponentials with the indicated time constants. *B*, Average time constant of current activation as a function of baclofen concentration. Points are mean ± SEM time constants for current activation (n = 10 at each concentration).

of agonist, there was no significant decline in current for ~150 msec. The lag in activation varied in different cells from 40 to 60 msec and that for deactivation from 150 to 200 msec.

The lags in activation and deactivation are consistent with a multi-step pathway involving agonist binding to receptor, activation of G-protein, and opening of K^+ channels. This suggests a complex temporal relationship between the presence of agonist and activation of current, especially for short applications of agonist. As shown in Figure 10, the current greatly outlasted the presence of agonist with short exposures. With a 200 msec baclofen application (Fig. 10*A*), current continued to rise after removal of agonist, so that peak current occurred approximately 150 msec later. With an even shorter application (for 60 msec), the conductance change did not even start until free agonist was no longer present (Fig. 10*B*), and it reached a peak 220 msec later.

In the experiments with short applications of agonist, we found that the deactivation of current was dependent on the length of agonist exposure. This effect is shown in Figure 11, in which baclofen was applied for different durations to a single cell. After the initial delay, the decline of current could be fit well by a single exponential in all cases. As the application length was increased, deactivation became progressively slower, changing from a time constant of 267 msec with a 200 msec application to a time constant of 721 msec after a 5 sec application. This effect was seen consistently.

Kinetics with GABA as agonist

We also examined currents activated by GABA, the natural agonist. The $GABA_B$ response was isolated by recording with 100 μM picrotoxin to block the $GABA_A$ response. Control experiments showed that 100 μM picrotoxin had no effect on current activated by 50 μM baclofen. Figure 12 compares in the same cell current activated by saturating concentrations of baclofen and GABA. Both the magnitude of current and the kinetics of activation and deactivation were essentially identical when elicited by GABA or baclofen. At saturating GABA concentrations, the activation time constant was 232 ± 17 msec (n = 13), and the deactivation time constant was 1.0 ± 0.2 sec (n = 14), very close to the values of 225 msec and 1.1 sec obtained with baclofen.

$GABA_B$- and $GABA_A$-activated currents compared

Both $GABA_B$ and $GABA_A$ receptors are present in the cell bodies of hippocampal CA3 neurons. We used the ability to apply well defined agonist concentrations to directly compare their sensitivity to GABA. The experiments in Figure 13 compare the kinetics and sensitivity of the two types of current, activated by 3 μM and 1 mM GABA. The $GABA_B$ response was recorded with 100 μM picrotoxin, and the $GABA_A$ current was recorded with 1 mM Ba^{2+} to block $GABA_B$ currents. The $GABA_B$-induced current was more sensitive to GABA, with 3 μM GABA activating more than half the maximal current activated by a saturating concentration of 1 mM GABA. As expected, the $GABA_B$ response was slower than the $GABA_A$ response, especially at 1 mM GABA, where the rise of the

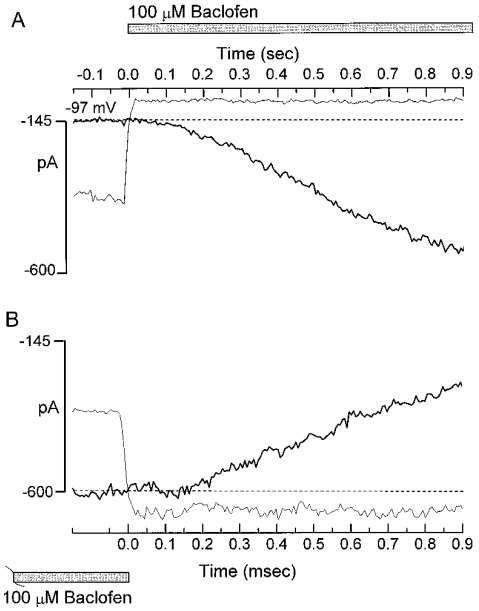

Figure 9. Lags in onset and offset of baclofen-activated current. Baclofen (100 μM) was applied for 3 sec at a holding potential of −97 mV with 60 mM external K^+. The onset of current (*A*) and offset of current (*B*) are shown at expanded time base. Four traces were signal-averaged (*thick line*). The precise timing of solution exchange around the cell was determined by switching from 60 mM external K^+ to 16 mM external K^+ in the continuous presence of 100 μM baclofen; four such calibration traces were signal-averaged (*thin line*). The calibration trace is shifted up by 100 pA to cross at time of onset and offset of baclofen.

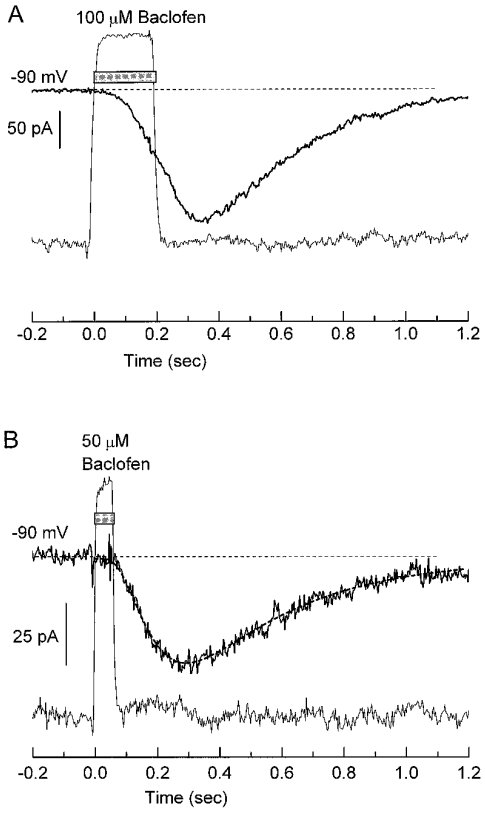

Figure 10. Current activation by short pulses of agonist. *A*, Baclofen (100 μM) was applied for 200 msec at −90 mV with 60 mM external K. Nine traces were signal-averaged (*thick line*). Timing of solution exchange was determined by switching from 60 mM external K^+ to 16 mM external K^+ (for 200 msec) in the continuous presence of 100 μM baclofen; six calibration traces were signal-averaged (*thin line*). The calibration trace is shifted up to cross the baclofen application trace. *Bar* indicating presence of baclofen corresponds to times at which change in calibrating current was 75% complete. *B*, Baclofen (50 μM) was applied for 60 msec at a holding potential of −92 mV with 60 mM external K. Four traces were signal-averaged (*thick line*), and four calibration traces were signal-averaged and shifted up (*thin trace*) to show timing of solution change. *Dashed curve* is drawn according to $(1 - \exp((t/\tau_m))4 \times \exp(t/\tau_h)$, with τ_m = 108 msec and τ_h = 365 msec, where t incorporates a 15 msec delay after the time of application (Otis et al., 1993).

$GABA_A$ response was as fast as the solution exchange. The deactivation of the $GABA_B$ response was also much slower than the $GABA_A$ response. In addition, desensitization of the $GABA_B$ response was far slower than that of the $GABA_A$ response. Figure 13*C* compares the magnitude and current–voltage relationship of the two responses when studied with physiological solutions and activated by saturating agonist concentrations. The $GABA_A$ response reversed significantly positive to the $GABA_B$ response and was far larger. The peak outward current elicited at −50 mV averaged 1280 ± 350 pA for the $GABA_A$ response and 50 ± 3 pA for the $GABA_B$ response.

Figure 14 shows a detailed comparison of the sensitivity of the $GABA_A$ and $GABA_B$ responses to GABA. GABA was much more potent in activating the $GABA_B$ response (EC_{50} 1.6 μM) than the $GABA_A$ response (25 μM). Figure 14*B* shows the result of experiments examining the apparent stoichiometry of the $GABA_B$ response at low GABA concentrations (0.1 −0.3 μM GABA). The current increased supralinearly with GABA concentration in all cells examined, with a Hill coefficient between 1.4 and 2.1 for individual cells (mean 1.66 ± 0.16, n = 4). Interestingly, the Hill coefficient was consistently higher when the response to this range of concentrations was smaller (relative to the current elicited by 100 μM GABA). This suggests that the variability in Hill coefficient between cells arises from variability in the position on the dose–response curve of the 0.1–0.3 μM range tested. Such variability could result from different ratios of receptor to G-protein or potassium channels. The $GABA_A$ response also had a supralinear response at GABA concentrations (in this case, 1–5 μM) that activated 0.003–0.2 of the maximal conductance. Both the relative potency of a given concentration and the Hill coefficient (1.70 ± 0.03; range, 1.6–1.8; n = 8) showed less variability than for the $GABA_B$ response, consistent with more direct coupling of ligand binding to channel activation.

The data on GABA dose dependence (Fig. 14) and current–voltage characteristics (Fig. 13*C*) of the two responses can be considered together to estimate the current that each response is capable of generating at low GABA concentrations with physiological ionic conditions. GABA at 0.3 μM activates ~0.1 of the maximal $GABA_B$ current (an average of +50 pA at −50 mV), yielding a 5 pA outward current. We could not directly measure any activation of $GABA_A$ current by 0.3 μM GABA, but extrapolating the relationships in Figure 14*C* predicts fractional activation of 0.0004. Even with the maximal current of +1280 pA for the peak $GABA_A$ response at −50 mV, the predicted current of 0.5 pA is lower than that for $GABA_B$ current. Thus, even though $GABA_A$ receptors can generate a far larger maximal current in our hippocampal neurons, the higher sensitivity of the $GABA_B$ response suggests that it carries more current at low GABA concentrations.

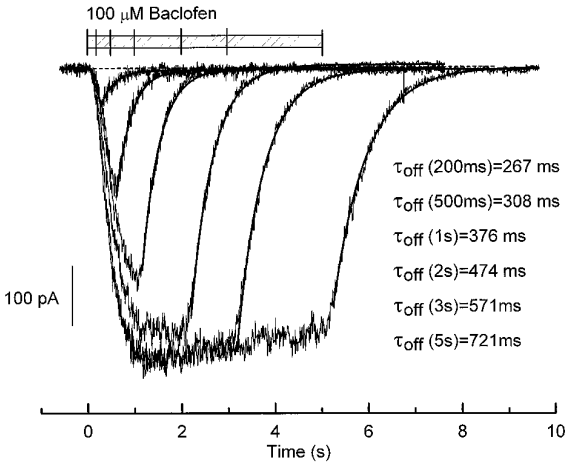

Figure 11. Change in deactivation rate with duration of agonist application. Inward current elicited from a single cell at a holding potential of −92 mV by 200 msec, 500 msec, and 1, 2, 3, and 5 sec applications of 100 μM baclofen. External solution: 60 mM K^+ Tyrode's solution. *Heavy lines* are fits to single exponentials with indicated time constants.

DISCUSSION

Block by Cs^+ and Ba^{2+}

All inwardly rectifying potassium channels are blocked by external Cs^+ and Ba^{2+} ions, but the properties of block differ among different types of channels. For example, block by Ba^{2+} is highly voltage dependent in some inward rectifiers (Standen and Stanfield, 1978; Hille, 1992a; Takano and Ashcroft, 1996). Ba^{2+} block of the $GABA_B$ receptor current was not voltage dependent, however. This corresponds to the behavior of acetylcholine-activated current in cardiac cells (Carmeliet and Mubagwa, 1986). Similarly, the potency of Ba^{2+} block in hippocampal neurons (EC_{50} 12 μM, Fig. 6) is virtually identical to that in cardiac tissue (2–18 μM) (Carmeliet and Mubagwa, 1986). Block by Cs^+ is also virtually identical in hippocampal neurons and cardiac tissue, in both potency and strong voltage dependence (compare Fig. 7 and Argibay et al., 1983).

Comparison with cloned channels

At least four members of the GIRK family of cDNAs, GIRK1, GIRK2, GIRK3, and CIR, are expressed in the hippocampus (Kobayashi et al., 1995; Lesage et al., 1995; Karschin et al., 1994, 1996; Ponce et al., 1996; Spauschus et al., 1996). Different

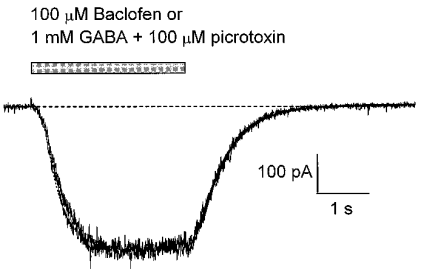

Figure 12. Similarity of kinetics with activation by baclofen and GABA. Current was elicited in the same neuron from a holding potential of −92 mV with 60 mM external K^+; 100 μM baclofen or 1 mM GABA was applied for 3 sec. For GABA application, both control and GABA solution contained 100 μM picrotoxin to inhibit $GABA_A$ receptor channels. *Solid lines* are exponential fits to activation (time constant 324 msec for baclofen, 315 msec for GABA) and deactivation (time constant 576 msec for baclofen, 583 msec for GABA).

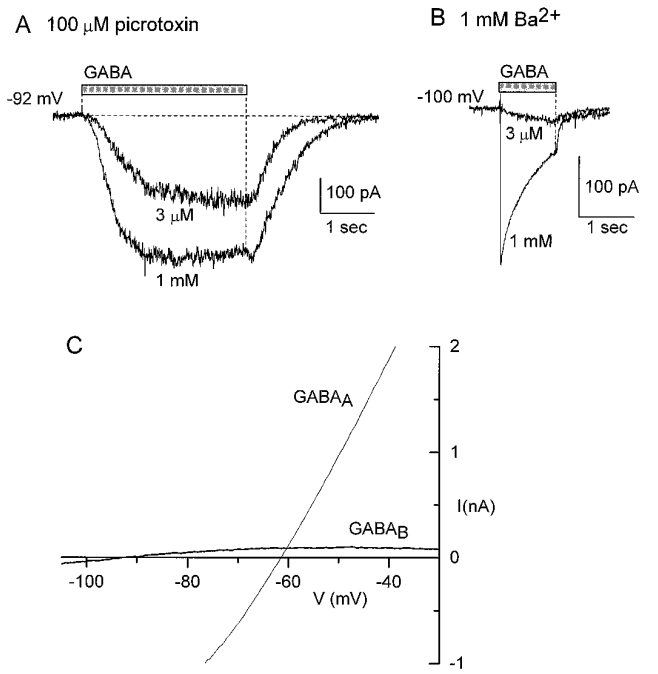

Figure 13. Comparison of GABA activation of $GABA_A$ and $GABA_B$ responses. *A*, Inward K current elicited by 3 sec applications of 3 μM and 1 mM GABA. External solution: 16 mM K^+ Tyrode's solution with 100 μM picrotoxin. Internal solution: 108 mM KH_2PO_4, 0.9 mM $MgCl_2$, 3.6 mM $MgSO_4$, 9 mM HEPES, 9 mM EGTA, 14 mM creatine phosphate (Tris salt), 4 mM Mg-ATP, and 0.3 mM GTP (Tris salt), pH-adjusted to 7.4 with 135.4 mM KOH. The $GABA_B$ reversal potential was −56 mV. *B*, Inward Cl^- current elicited at a holding potential of −100 mV by 1 sec applications of 3 μM and 1 mM GABA. External solution: 16 mM K^+ modified Tyrode's solution with 1 mM Ba^{2+}. Internal solution as in *A*. Reversal potential for $GABA_A$ response was −92 mV. *C*, Comparison of magnitude and current–voltage relationship for $GABA_B$ and $GABA_A$ responses with quasi-physiological ionic conditions. External solution: Tyrode's solution with 4 mM K^+. Internal solution: 108 mM KH_2PO_4, 4.5 mM $MgCl_2$, 9 mM HEPES, 9 mM EGTA, 14 mM creatine phosphate (Tris salt), 4 mM Mg-ATP, and 0.3 mM GTP (Tris salt), pH adjusted to 7.4 with 135.4 mM KOH. $GABA_B$ response elicited by 100 μM baclofen and $GABA_A$ response (in a different cell) by 1 mM GABA, with 1 mM $BaCl_2$ added to external solution to block $GABA_B$ response.

GIRK proteins combine to form multimeric channels (Duprat et al., 1995; Kofuji et al., 1995; Krapivinsky et al., 1995a; Lesage et al., 1995; Spauschus et al., 1996). Native G-protein-activated channels in heart include GIRK1 and CIR subunits (Krapivinsky et al., 1995a). The subunit composition of native G-protein-activated channels in hippocampal neurons is not yet known, but the single-channel properties of GIRK1/GIRK2 channels (Velimirovic et al., 1996) resemble those of G-protein-gated channels in neurons (Miyake et al., 1989; Penington et al., 1993b; Oh et al., 1995; Grigg et al., 1996). The rectification properties that we found in CA3 neurons, with substantial outward current, correlate better with GIRK1/GIRK2 (Velimirovic et al., 1996) or GIRK1/CIR (Krapivinsky et al., 1995a; Spauschus et al., 1996) channels than with monomeric GIRK1 channels, which rectify so strongly that there is essentially no outward current (Dascal et al., 1993; Kubo et al., 1993). So far, none of the multimeric cloned channels demonstrate block by Ba^{2+} similar to that in native CA3 neuron channels (EC_{50} 12 μM with no voltage dependence). Both GIRK1/CIR (Krapivinsky et al., 1995a) and GIRK1/GIRK2 (Velimirovic et al., 1996) channels have much lower Ba^{2+} sensitivity (EC_{50} ~500 μM),

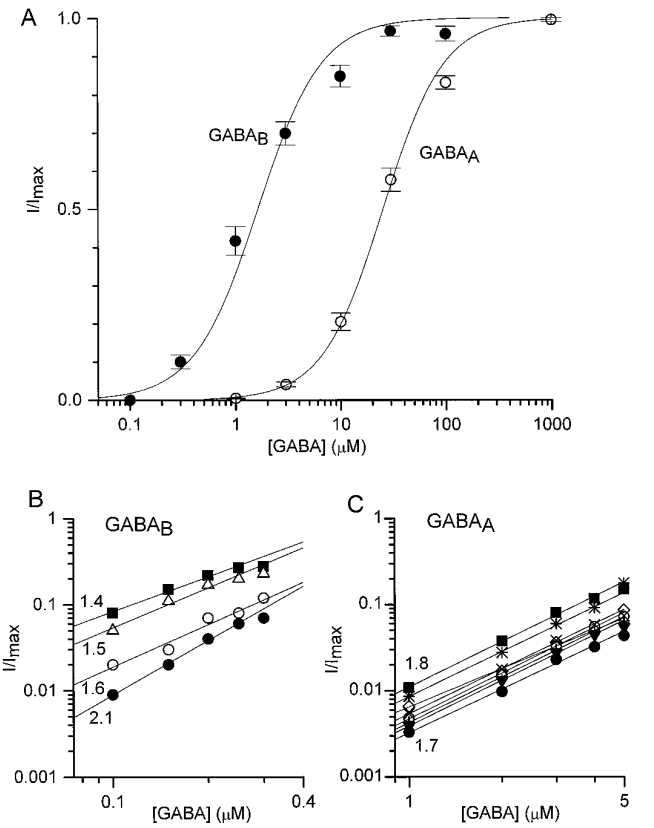

Figure 14. Dose dependence for GABA activation of $GABA_B$ and $GABA_A$ responses. *A*, Dose–response relationships for $GABA_B$ (*closed circles*; mean ± SEM for 9 cells) and for $GABA_A$ (*open circles*; mean ± SEM for 6 cells). Dose–response relationships were determined in the absence of blockers and in identical external and internal solutions by measuring the $GABA_B$ response at the reversal potential for $GABA_A$ current and the $GABA_A$ response at the reversal potential for $GABA_B$ current. The solutions for these experiments [external: modified Tyrode's solution with 16 mM K^+; internal: 108 mM KH_2PO_4, 0.9 mM $MgCl_2$, 3.6 mM $MgSO_4$, 9 mM HEPES, 9 mM EGTA, 14 mM creatine phosphate (Tris salt), 4 mM Mg-ATP, and 0.3 mM GTP (Tris salt), pH adjusted to 7.4 with 135.4 mM KOH] were chosen so that the $GABA_B$ reversal potential (−56 ± 1 mV; n = 7) was well separated from the $GABA_A$ reversal potential (−92 ± 0.2 mV; n = 9). Reversal potentials were determined using voltage ramps from −172 to −40 mV. The $GABA_B$ reversal potential was defined by baclofen application. The rapid desensitization of the $GABA_A$ response with 1 mM GABA was used to determine its reversal potential: as the response desensitized, the ramp trace pivoted around the reversal potential. The response at each GABA concentration was normalized to the maximal response obtained with 100 μM or 1 mM GABA. The full series of six or seven agonist concentrations was preceded and followed by application of 100 μM GABA, and results were used only if these responses differed by <20%. The lines are the best least-squares fit to $1/(1 + (EC_{50}/[GABA])^n)$, where EC_{50} is the half-maximally effective concentration of GABA. $GABA_B$: EC_{50} = 1.6 μM, n = 1.4; $GABA_A$: EC_{50} = 25 μM, n = 1.5. *B*, Dose dependence of $GABA_B$ responses at low GABA concentrations. $GABA_B$-activated current was elicited by successive application of 0.1–0.3 μM GABA in 0.05 μM increments. Each *symbol* shows data from a different cell. *Straight lines* are fit to points at four lowest GABA concentrations and have indicated slopes. Solutions as in *A* but with 100 μM picrotoxin added to external solutions. *C*, Dose dependence of $GABA_A$ responses at low GABA concentrations. $GABA_A$-activated current elicited at −90 mV by application of 1–5 μM GABA; 1 mM Ba^{2+} in external solutions blocked $GABA_B$ responses. External solution: 4 mM K^+ Tyrode's. Internal solution: 112.5 mM CsCl, 4.5 mM $MgCl_2$, 9 mM HEPES, 9 mM EGTA, 14 mM creatine phosphate (Tris salt), 4 mM Mg-ATP, 0.3 mM GTP (Tris salt), pH adjusted to 7.4 with CsOH.

and block of both is strongly voltage dependent (Spauschus et al., 1996; Velimirovic et al., 1996). Thus, the voltage dependence and sensitivity of Ba^{2+} block of native channels are quite different than any combination of subunits yet described. Possibly, native channels have additional subunits to those so far known.

Voltage-dependent relaxations

The $GABA_B$ receptor-activated current showed no time-dependent relaxations with voltage steps (Fig. 7), which was different from muscarinic receptor-activated current in cardiac myocytes (Noma and Trautwein, 1978; Simmons and Hartzell, 1987; Clark et al., 1990). GIRK1 forms channels that show prominent voltage-dependent relaxations, regardless of whether current is activated by various G-protein-linked receptors or by coexpressed $\beta\gamma$ G-protein subunits (Kubo et al., 1993; Doupnik et al., 1995; Krapivinsky et al., 1995a). Similar voltage-dependent gating of other inward-rectifier channels results from time- and voltage-dependent block and unblock by intracellular spermine or a related polyamine (Ficker et al., 1994; Lopatin et al., 1994; Fakler et al., 1995), and polyamines can interact similarly with cloned GIRK1 channels (Yamada and Kurachi, 1995). It is possible that hippocampal neurons have lower concentrations of such polyamines than oocytes or cardiac myocytes. In principle, endogenous polyamines may have been dialyzed out of the neurons by our whole-cell recording, but the baclofen-induced current in undialyzed hippocampal neurons studied with sharp microelectrode recording also showed no obvious time dependence during hyperpolarizations (Gähwiler and Brown, 1985). The difference from myocytes could also reflect different subunit composition of the channels, which influences the relaxations (Kofuji et al., 1995; Lesage et al., 1995; Velimirovic et al., 1996).

Kinetics

Our experiments provide the first description of the kinetics of $GABA_B$ receptor-activated current with rapid application and removal of agonist. As with the kinetics of $GABA_B$ receptor inhibition of calcium current (Pfrieger et al., 1994), activation and deactivation take hundreds of milliseconds, far slower than for channels directly activated by ligand binding. The limiting rate of channel activation at high ligand concentrations was ~4 sec^{-1}, which can be compared with 4000 sec^{-1} for $GABA_A$ receptor chloride channels (Maconochie et al., 1994). Reasonable candidates for the rate-limiting step in $GABA_B$ receptor activation of potassium channels include GDP/GTP exchange, diffusion of activated G-protein to the channel, and channel activation by activated G-protein. Consistent with a multi-step pathway, the main rising phase of current was preceded by a lag of ~50 msec; similar lags have been seen for potassium current activated by acetylcholine in myocytes (~80 msec; Inomata et al., 1989) and by noradrenaline in submucosus plexus neurons (~60 msec; Surprenant and North, 1988). The time constant for the main phase of the off response (0.2–1.0 sec, depending on duration of exposure) is also similar to that for other G-protein-mediated conductances: 0.3–2.0 sec for atrial cells (Breitwieser and Szabo, 1988; Friel and Bean, 1990) and 0.15–0.2 sec for submucosus plexus neurons (Surprenant and North, 1988). The off response may well be limited by the rate of GTP hydrolysis, estimated by Breitwieser and Szabo (1988) to be ~1 sec^{-1} in atrial cells. The dependence of the off rate on the duration of agonist application has not been noted previously for G-protein-activated K^+ currents, and its origin is unclear.

The effect could arise if the K^+ channels can bind more $\beta\gamma$ subunits than are needed to produce channel activation. A requirement for unbinding of multiple $\beta\gamma$ subunits could contribute to the lag in deactivation as well.

Comparison with synaptically activated currents

The current activated by short pulses of agonist is almost identical in kinetics to the $GABA_B$-mediated synaptic currents recorded by Otis et al. (1993) in granule neurons. The current in Figure 10*B* activated by a 60 msec application of baclofen could be fit very well (*dashed line*) with m^4h kinetics (Otis et al., 1993). The fit gave τ_m of 108 msec and τ_h of 345 msec, similar to their average values of 112 and 282 msec (for the main component of decay) for synaptic currents at 22–23°C. The comparison suggests that the slow kinetics of synaptic currents can be accounted for entirely by the time course of receptor-to-channel coupling.

Because the synaptically activated $GABA_B$ conductance does not show inward rectification (Thalmann, 1988; Otis et al., 1993), the possibility was raised that the rectification of baclofen-induced current reflects inadequately voltage-clamped cells in slice recordings (Otis et al., 1993). Because our recordings were performed with cells that can be voltage-clamped beyond reproach, this possibility can be ruled out. The reason for the nonrectification of synaptically activated current remains a puzzle; perhaps intracellular levels of either polyamines or Mg^{2+} are lower near dendritic receptors.

Dose–response and $GABA_B$ versus $GABA_A$ sensitivity

Our results provide the first measurements of the sensitivity of $GABA_B$ receptor-activated current to well defined low concentrations of GABA. They show that the EC_{50} for activation of potassium current is much lower (1.6 μM) than for activation of $GABA_A$ receptor chloride channels (25 μM) in the same cells. Most likely, $GABA_B$ receptors have significantly higher affinity for GABA than do $GABA_A$ receptors, although the functional EC_{50} may be lower if there are "spare" $GABA_B$ receptors. In any case, the high sensitivity to low GABA concentrations supports the idea that $GABA_B$ receptor-activated current may be readily activated by diffuse "spill-over" of GABA from synapses (Thompson and Gähwiler, 1992b; Isaacson et al., 1993; Mody et al., 1994). In fact, the current was significantly activated by GABA in the range of 0.1–0.4 μM, within the range estimated for basal extracellular GABA (0.8 μM, Lerma et al., 1986; 0.2 μM, Tossman et al., 1986). This suggests that only minimal increases are needed.

We found that the dose–response relationship at low GABA concentrations is nonlinear, with a Hill coefficient of 1.7. To our knowledge this is the first demonstration of a nonlinear relationship in agonist activation of a G-protein-coupled conductance [cf. Breitwieser and Szabo, 1988; Inomata et al., 1989; Hille, 1992b; see Destexhe and Sejnowski (1995) for a model incorporating stronger supralinearity]. The supralinearity implies cooperativity at some stage in the coupling pathway. Unlike the $GABA_A$ current, which has an identical Hill coefficient, the cooperativity is unlikely to arise at the receptor level. A likely step for cooperativity is the activation of channels by $\beta\gamma$ subunits; in atrial mycocyte channels, activation by various $\beta\gamma$ subunits yielded an average Hill coefficient of 1.5 (Krapivinsky et al., 1995b), although values as high as 3 have been found for particular $\beta\gamma$ combinations (Ito et al., 1992; Krapivinsky et al., 1995b).

It is a long-standing observation that $GABA_B$-mediated inhibitory postsynaptic potentials require stronger or more sustained stimulation than $GABA_A$-mediated responses do. Our results show that this occurs despite a much higher sensitivity of $GABA_B$ receptors to GABA. The failure of $GABA_B$ receptors to be activated by synaptic stimulation capable of activating $GABA_A$ receptors argues strongly for different localization of the two receptor types, with $GABA_A$ receptors located immediately postsynaptically and $GABA_B$ receptors located primarily extrasynaptically, as has been proposed (Thompson and Gähwiler, 1992b; Isaacson et al., 1993). The high sensitivity of $GABA_B$ receptors makes them well suited to respond to extrasynaptic GABA.

REFERENCES

Andrade R, Malenka RC, Nicoll RA (1986) A G protein couples serotonin and $GABA_B$ receptors to the same channels in hippocampus. Science 234:1261–1265.

Andrade R, Nicoll RA (1987) Pharmacologically distinct actions of serotonin on single pyramidal neurones of the rat hippocampus recorded in vitro. J Physiol (Lond) 394:99–124.

Argibay JA, Dutey P, Ildefonse M, Ojeda C, Rougier O, Tourneur Y (1983) Block by Cs of K current i_{K1} and of carbachol induced K current i_{Cch} in frog atrium. Pflügers Arch 397:295–299.

Breitwieser GE, Szabo G (1988) Mechanism of muscarinic receptor-induced potassium channel activation as revealed by hydrolysis-resistant GTP analogues. J Gen Physiol 91:469–493.

Carmeliet E, Mubagwa K (1986) Changes by acetylcholine of membrane currents in rabbit cardiac Purkinje fibres. J Physiol (Lond) 371:201–217.

Clark RB, Nakajima T, Giles W, Kanai K, Momose Y, Szabo G (1990) Two distinct types of inwardly rectifying K channels in bullfrog atrial myocytes. J Physiol (Lond) 424:229–251.

Dascal N, Schreibmayer W, Lim NF, Wang W, Chavkin C, DiMagno L, Labarca C, Kieffer BL, Gaveriaux-Ruff C, Trollinger D, Lester HA, Davidson N (1993) Atrial G-protein-activated K^+ channel: expression cloning and molecular properties. Proc Natl Acad Sci USA 90:10235–10239.

Destexhe A, Sejnowski T (1995) G protein activation kinetics and spill-over of γ-aminobutyric acid may account for differences between inhibitory responses in the hippocampus and thalamus. Proc Natl Acad Sci USA 92:9515–9519.

Doupnik CA, Lim NF, Kofuji P, Davidson N, Lester HA (1995) Intrinsic gating properties of a cloned G protein-activated inward rectifier K channel. J Gen Physiol 106:1–23.

Duprat F, Lesage F, Guillemare E, Fink M, Hugnot JP, Bigay J, Lazdunski M, Romey G, Barhanin J (1995) Heterologous multimeric assembly is essential for K channel activity of neuronal and cardiac G-protein-activated inward rectifiers. Biochem Biophys Res Commun 12:657–663.

Dutar P, Nicoll RA (1988) A physiological role for $GABA_B$ receptors in the central nervous system. Nature 332:156–158.

Fakler B, Brandle U, Glowatzki E, Weidemann S, Zenner HP, Ruppersberg JP (1995) Strong voltage-dependent inward rectification of inward rectifier K channels is caused by intracellular spermine. Cell 80:149–154.

Ficker E, Taglialatela M, Wible BA, Henley CM, Brown AM (1994) Spermine and spermidine as gating molecules for inward rectifier K channels. Science 266:1068–1072.

Friel DD, Bean BP (1990) Dual control by ATP and acetylcholine of inwardly rectifying potassium channels in bovine atrial cells. Pflügers Arch 415:651–657.

Gähwiler BH, Brown DA (1985) $GABA_B$-receptor-activated potassium current in voltage-clamped CA3 pyramidal cells in hippocampal cultures. Proc Natl Acad Sci USA 82:1558–1562.

Grigg JJ, Kozasa T, Nakajima Y, Nakajima S (1996) Single-channel properties of a G-protein-coupled inward rectifier potassium channel in brain neurons. J Neurophysiol 75:318–328.

Harrison NL (1990) On the presynaptic action of baclofen at inhibitory synapses between cultured rat hippocampal neurones. J Physiol (Lond) 422:433–446.

Hartzell HC (1988) Regulation of cardiac ion channels by catecholamines, acetylcholine and second messenger systems. Prog Biophys Mol Biol 52:165–247.

Harvey RD, Ten Eick RE (1989) Voltage-dependent block of cardiac inward rectifying potassium current by monovalent cations. J Gen Physiol 94:349–361.

Hille B (1992a) Ionic channels of excitable membranes. Sutherland, MA: Sinauer.

Hille B (1992b) G protein-coupled mechanisms and nervous signalling. Neuron 9:187–195.

Huang C-L, Slesinger PA, Casey PJ, Jan YN, Jan LY (1995) Evidence that direct binding of $G\beta\gamma$ to the GIRK1 G protein-gated inwardly rectifying channel is important for channel activation. Neuron 15:1133–1143.

Inanobe A, Morishige K, Takahashi N, Ito H, Mitsuhiko Y, Takumi T, Nishina H, Takahashi K, Kanaho Y, Katada T, Kurachi Y (1995) $G\beta\gamma$ directly binds to the carboxyl terminus of the G protein-gated muscarinic K channel, GIRK1. Biochem Biophys Res Commun 212:1022–1028.

Inomata N, Ishihara T, Akaike N (1989) Activation kinetics of the acetylcholine-gated potassium current in isolated atrial cells. Am J Physiol 257:C646–C650.

Isaacson JS, Solis JM, Nicoll RA (1993) Local and diffuse actions of GABA in the hippocampus. Neuron 10:165–175.

Ito H, Sugimoto T, Kobayashi I, Takahashi K, Katada T, Ui M, Kurachi Y (1991) On the mechanism of basal and agonist-induced activation of the G protein-gated muscarinic potassium channel in atrial myocytes of guinea pig heart. J Gen Physiol 98:517–533.

Ito H, Tung RT, Sugimoto T, Kobayashi I, Takahashi K, Katada T, Ui M, Kurachi Y (1992) On the mechanism of G protein $\beta\gamma$ subunit activation of the muscarinic K^+ channel in guinea pig atrial cell membrane. J Gen Physiol 99:961–983.

Karschin C, Schreibmayer W, Dascal N, Lester H, Davidson N, Karschin A (1994) Distribution and localization of a G protein-coupled inwardly rectifying K channel in the rat. FEBS Lett 348:139–144.

Karschin C, Dißmann E, Stühmer W, Karschin A (1996) IRK(1–3) and GIRK(1–4) inwardly rectifying K^+ channel mRNAs are differentially expressed in the adult rat brain. J Neurosci 16:3559–3570.

Kobayashi T, Ikeda K, Ichikawa T, Abe S, Togashi S, Kumanishi T (1995) Molecular cloning of a mouse G-protein-activated K channel (mGIRK1) and distinct distributions of three GIRK (GIRK1, 2 and 3) mRNAs in mouse brain. Biochem Biophys Res Commun 208:1166–1173.

Kofuji P, Davidson N, Lester HA (1995) Evidence that neuronal G-protein-gated inwardly rectifying K channels are activated by $G\beta\gamma$ subunits and function as heteromultimers. Proc Natl Acad Sci USA 92:6542–6546.

Krapivinsky G, Gordon EA, Wickmann K, Velimirovic B, Krapivinsky L, Clapham DE (1995a) The G-protein-gated atrial K channel IkACh is a heteromultimer of two inwardly rectifying K-channel proteins. Nature 374:135–141.

Krapivinsky G, Krapivinsky L, Wickman K, Clapham DE (1995b) $G\beta\gamma$ binds directly to the G protein-gated K channel, IkACh. J Biol Chem 270:29059–29062.

Kubo Y, Reuveny E, Slesinger PA, Jan YN, Jan LY (1993) Primary structure and functional expression of a rat G-protein-coupled muscarinic potassium channel. Nature 364:802–806.

Kurachi Y, Nakajima T, Sugimoto T (1986a) Acetylcholine activation of K^+ channels in cell-free membrane of atrial cells. Am J Physiol 251:H681–H684.

Kurachi Y, Nakajima T, Sugimoto T (1986b) On the mechanism of activation of muscarinic K channels by adenosine in isolated atrial cells: involvement of GTP-binding proteins. Pflügers Arch 407:264–274.

Lerma J, Herranz AS, Herreras O, Abraira V, Martin del Rio R (1986) In vivo determination of extracellular concentrations of amino acids in the rat hippocampus: a method based on brain dialysis and computerized analysis. Brain Res 384:145–155.

Lesage F, Duprat F, Fink M, Guillemare E, Coppola T, Lazdunski M, Hugnot JP (1994) Cloning provides evidence for a family of inward rectifier and G-protein coupled K channels in the brain. FEBS Lett 353:37–42.

Lesage F, Guillemare E, Fink M, Duprat F, Heurteaux C, Fosset M, Romey G, Barhanin J, Lazdunski M (1995) Molecular properties of neuronal G-protein-activated inwardly rectifying K channels. J Biol Chem 270:28660–28667.

Logothetis DE, Kurachi Y, Galper J, Neer EJ, Clapham DE (1987) The $\beta\gamma$ subunits of GTP-binding proteins activate the muscarinic potassium channel in heart. Nature 325:321–326.

Lopatin AN, Makhina EN, Nichols CG (1994) Potassium channel block by cytoplasmic polyamines as the mechanism of intrinsic rectification. Nature 372:366–369.

Maconochie DJ, Zempel JM, Steinbach JH (1994) How quickly can $GABA_A$ receptors open? Neuron 12:61–71.

McDonough SI, Swartz KJ, Mintz IM, Boland LM, Bean BP (1996) Inhibition of calcium channels in rat central and peripherals neurons by ω-conotoxin MVIIC. J Neurosci 16:2612–2623.

Misgeld U, Muller W, Brunner H (1989) Effects of (−)baclofen on inhibitory neurons in the guinea pig hippocampal slice. Pflügers Arch 414:139–144.

Miyake M, Christie MJ, North RA (1989) Single potassium channels opened by opioids in rat locus ceruleus neurons. Proc Natl Acad Sci USA 86:3419–3422.

Mody I, De Koninck Y, Otis TS, Soltesz I (1994) Bridging the cleft at GABA synapses in the brain. Trends Neurosci 17:517–525.

Nakajima T, Irisawa H, Giles W (1990) *N*-Ethylmaleimide uncouples muscarinic receptors from Ach-sensitive K channels in bullfrog atrium. Biophys J 57:110a.

Neher E (1992) Correction for liquid junction potentials in patch clamp experiments. Methods Enzymol 207:123–131.

Newberry NR, Nicoll RA (1985) Comparison of the action of baclofen with γ-aminobutyric acid on rat hippocampal pyramidal cells in vitro. J Physiol (Lond) 360:161–185.

Nicoll RA, Malenka RM, Kauer JA (1990) Functional comparison of neurotransmitter receptor subtypes in mammalian central nervous system. Physiol Rev 70:513–565.

Noma A, Trautwein W (1978) Relaxation of the ACh-induced potassium current in the rabbit sinoatrial node. Pflügers Arch 377:193–200.

North RA (1989) Drug receptors and the inhibition of nerve cells. Br J Pharmacol 98:13–28.

North RA, Williams JT, Surprenant A, Christie MJ (1987) μ and δ receptors belong to a family of receptors that are coupled to potassium channels. Proc Natl Acad Sci USA 84:5487–5491.

Oh U, Ho Y-K, Kim D (1995) Modulation of the serotonin-activate K^+ channel by G protein subunits and nucleotides in rat hippocampal neurons. J Membr Biol 147:241–253.

Ohmori H (1978) Inactivation kinetics and steady-state current noise in the anomolous rectifier of tunicate egg cell membranes. J Physiol (Lond) 383:231–249.

Otis TS, Mody I (1992) Differential activation of $GABA_A$ and $GABA_B$ by spontaneously released transmitter. J Neurophysiol 67:227–235.

Otis TS, DeKoninck Y, Mody I (1993) Characterization of synaptically elicited $GABA_B$ responses using patch clamp recordings in rat hippocampal slices. J Physiol (Lond) 463:391–407.

Penington N, Kelly JS, Fox AP (1993a) Whole-cell recordings of inwardly-rectifying K^+ currents activated by 5-HT1A receptors on dorsal raphe neurones of the adult rat. J Physiol (Lond) 469:387–405.

Penington N, Kelly JS, Fox AP (1993b) Unitary properties of potassium channels activated by 5-HT in acutely-isolated rat dorsal raphe neurones. J Physiol (Lond) 469:406–426.

Pfaffinger PJ, Martin JM, Hunter DD, Nathanson NM, Hille B (1985) GTP-binding proteins couple cardiac muscarinic receptors to a K channel. Nature 317:536–538.

Pfrieger F, Gottmann K, Lux HD (1994) Kinetics of $GABA_B$ receptor-mediated inhibition of calcium currents and excitatory synaptic transmission in hippocampal neurons in vitro. Neuron 12:97–107.

Ponce A, Bueno E, Kentros C, Miera EV, Chow A, Hillman D, Chen S, Zhu L, Wu MB, Wu X, Rudy B, Thornhill WB (1996) G-protein-gated inward rectifier K channel proteins (GIRK1) are present in the soma and dendrites as well as in the nerve terminals of specific neurons in the brain. J Neurosci 16:1990–2001.

Reuveny E, Slesinger PA, Inglese J, Morales JM, Iniguez-Lluhi JA, Lefkowitz RJ, Bourne HR, Jan YN, Jan LY (1994) Activation of the cloned muscarinic potassium channel by G protein $\beta\gamma$ subunits. Nature 370:143–146.

Robinson RA, Stokes RH (1959) Electrolyte solutions, 2nd edition. London: Butterworths.

Sakmann B, Noma A, Trautwein W (1983) Acetylcholine activation of single muscarinic K channels in isolated pacemaker cells of the mammalian heart. Nature 303:250–253.

Schreibmayer W, Dessauer CW, Vorobiov D, Gilman AG, Lester HA, Davidson N, Dascal N (1996) Inhibition of an inwardly rectifying K^+ channel by G-protein α-subunits. Nature 380:624–627.

Simmons MA, Hartzell HC (1987) A quantitative analysis of the acetylcholine-activated potassium current in single cells from frog atrium. Pflügers Arch 409:454–461.

Spauschus A, Lentes KU, Wischmeyer E, Dibmann E, Karschin C, Karschin A (1996) A G-protein-activated inwardly rectifying K channel (GIRK4) from human hippocampus associates with other GIRK channels. J Neurosci 16:930–938.

Standen NB, Stanfield PR (1978) A potential and time-dependent blockade of inward rectification in frog skeletal muscle fibres by barium and strontium ions. J Physiol (Lond) 280:169–191.

Standen NB, Stanfield PR (1979) Potassium depletion and sodium block of potassium currents under hyperpolarization in frog sartorius muscle. J Physiol (Lond) 294:497–520.

Surprenant A, North RA (1988) Mechanism of synaptic inhibition by noradrenaline acting at α_2-adrenoceptors. Proc R Soc Lond [Biol] 234:85–114.

Takano M, Ashcroft FM (1996) The Ba^{2+} block of the ATP-sensitive K^+ current of mouse pancreatic B-cells. Pflügers Arch 431:625–631.

Thalmann RH (1988) Evidence that GTP-binding proteins control a synaptic response in brain: effect of pertussis toxin and GTPγS on the late inhibitory postsynaptic potential of hippocampal CA3 neurons. J Neurosci 8:4589–4602.

Thompson SM, Gähwiler BH (1992a) Comparison of the actions of baclofen at pre- and postsynaptic receptors in the rat hippocampus in vitro. J Physiol (Lond) 451:329–345.

Thompson SM, Gähwiler BH (1992b) Effects of the GABA uptake inhibitor tiagabine in inhibitory synaptic potentials in rat hippocampal slice cultures. J Neurophysiol 67:1698–1701.

Tossman U, Jonsson G, Ungerstedt U (1986) Regional distribution and extracellular levels of amino acids in rat central nervous system. Acta Physiol Scand 127:533–545.

Velimirovic BM, Gordon EA, Lim NF, Navarro B, Clapham DE (1996) The K channel inward rectifier subunits form a channel similar to neuronal G protein-gated K channel. FEBS Lett 379:31–37.

Wickman KD, Iniguez-Lluhi JA, Davenport PA, Taussig R, Krapivinsky GB, Linder ME, Gilman AG, Clapham DE (1994) Recombinant G protein $\beta\gamma$-subunits activate the muscarinic-gated atrial potassium channel. Nature 368:255–257.

Wollmuth LP, Shapiro MS, Hille B (1995) Pancreatic polypeptide inhibits calcium channels in rat sympathetic neurons via two signalling pathways. J Neurophysiol 73:1323–1328.

Yamada M, Kurachi Y (1995) Spermine gates inward-rectifying muscarinic but not ATP-sensitive K^+ channels in rabbit atrial myocytes. J Biol Chem 270:9289–9294.

Yoon K-W, Rothman SM (1991) The modulation of rat hippocampal synaptic conductances by baclofen and γ-aminobutyric acid. J Physiol (Lond) 442:377–390.